Characterization of the blue-light activated adenylyl cyclase mPAC by flash photolysis and FTIR spectroscopy

Silke Kerruth[1], Pit Langner[1], Sarah Raffelberg[2], Wolfgang Gärtner[3] und Joachim Heberle[1*]

[1]Freie Universität Berlin, Experimental Molecular Biophysics, Arnimallee 14, 14195 Berlin, Germany.

[2] University of Geneva, Department of Botany and Plant Biology, 30 Quai E. Ansermet, 1211 Geneva, Switzerland.

[3]Max Planck Institute for Chemical Energy Conversion, Stiftstr. 34-36, 45470 Mühlheim a. d. Ruhr, Germany.

*Corresponding author:

Tel: +49-30-838-56164

Fax: +49-30-838-56510

email: joachim.heberle@fu-berlin.de

KEYWORDS

flavoprotein, LOV, optogenetics, photoreceptor

ABSTRACT

The recently discovered photo-activated adenylyl cyclase (mPAC from *Microcoleus chthonoplastes)* is the first PAC that owes a light-, oxygen- and voltage sensitive (LOV) domain for blue-light sensing. The photoreaction of the mPAC receptor was studied by time-resolved UV/Vis and light-induced Fourier-transform infrared (FTIR) absorption difference spectroscopy. The photocycle comprises of the typical triplet state LOV_{715} and the thio-adduct state LOV_{390}. While the adduct state decays with a time constant of 8 s, the lifetime of the triplet state is with 656 ns significantly shorter than in all other reported LOV domains. The light-induced FTIR difference spectrum shows the typical bands of the LOV_{390} and LOV_{450} intermediates. The negative S-H stretching vibration at 2573 cm^{-1} is asymmetric suggesting two rotamer configurations of the protonated side chain of C197. A positive band at 3636 cm^{-1} is observed, which is assigned to an internal water molecule. In contrast to other LOV domains, mPAC exhibits a second positive feature at 3674 cm^{-1} which is due to the O-H stretch of a second intrinsic water molecule and the side chain of Y476. We conclude that the latter might is involved in the dimerization of the cyclase domain which is crucial for ATP binding.

INTRODUCTION

Blue and ultraviolet light is the wavelength range with the highest energy of the sun's emission that reaches the surface of the earth. These light qualities are ambivalent for living organisms. They can be employed as high energy sources, but both blue and ultraviolet light can cause severe damage in tissue and in biological macromolecules such as DNA or proteins, in a direct manner or via generation of singlet oxygen and other ROS. Accordingly, nearly all organisms have developed proteins during evolution to detect this high energy light in order to adapt their lifestyle in response to irradiation intensity or duration. In many cases, these blue-light (BL) sensitive receptors use flavin derivatives as chromophores (1).

Besides many others, e.g., histidine kinases, DNA-binding motifs or phosphodiesterases, adenylyl cyclases were recently added to the broad variety of light-regulated signaling domains. Furthermore, the identification of flavoproteins carrying adenylyl cyclases (PAC) (2), opened a new drawer in the toolbox of optogenetics, as in particular cAMP and to a lesser extent cGMP are major players in many metabolic pathways. Schröder-Lang et al. (3) demonstrated in an *in vivo* experiment that the cellular level of the second messenger cAMP can be rapidly changed by light. The functional expression in various cells like oocytes from *Xenopus laevis* (3), bacteria, fruit flies and rodent neurons and their manipulation by light identified PACs as powerful optogenetic tools.

The receptors that mediate photophobic response in the unicellular flagellate *Euglena gracilis*, were named PACα and PACβ. These proteins comprise two flavin adenine dinucleotide (FAD) binding domains, F1 and F2, belonging to the family of BLUF (blue-light using FAD) domains, each of which being fused to a catalytic adenylyl cyclase (AC) domains, C1 and C2. These AC domains show homology to class III adenylyl cyclases and form intermolecular heterodimers with two putative substrate binding sites (4). Illumination with blue-light leads to a fast increase (within seconds (5, 3)) in cAMP level with an 80-fold higher cyclase activity in the light (2). A bacterial photo-activated adenylyl cyclase was found in *Beggiatoa* (6). bPAC consists of a single BLUF with a downstream AC domain. With 350 amino acids, it is of much smaller size than PAC from *Euglena*. bPAC shows a 300-fold increase in cyclase activity upon light activation and decays thermally within 13 s. Furthermore, it was shown that bPAC produces large inward currents when expressed parallel to

cAMP dependent channels in oocytes (6). Recently, a new form of photo-activated adenylyl cyclases was found in *Microcoleus chthonoplastes* (7). This receptor, called mPAC, uses a LOV (light-, oxygen- and voltage-sensitive) domain for blue-light sensing and shows comparable light sensitivity to bPAC. Although the increase of activity under BL irradiation is only 30-fold, its overall higher constitutive activity in the dark as well as in light reveals in much higher cAMP levels in cells and, thus, to a better response (7).

LOV domains belong to the Per-ARNT-Sim (PAS) superfamily with its classical α,β fold, consisting of a five-stranded anti-parallel β-sheet and four helices (8). Within this fold a flavin mononucleotide (FMN) is non-covalently bound that acts as chromophore. Absorption of a blue photon by FMN of ground state LOV, LOV_{445}, leads to the electronically excited state which decays within a few nanoseconds via intersystem crossing to the triplet state, LOV_{715} (9). The triplet state decays subsequently with a time constant of a few microseconds into the adduct state $LOV_{390,}$ most probably via a neutral radical mechanism (10). This intermediate is characterized by a covalent bond that is formed between the C(4a) of the isoallaxazine ring of the FMN and the terminal sulfur of a nearby cysteine (11, 9). Due to strained protein conformation, adduct state decays thermally into the ground state LOV_{445}. This decay strongly varies among the large family of LOV domains and covers the time range from seconds to hours (12, 11, 13, 14).

Associated with the photo activity of the chromophore are structural changes of the apo-protein. Fourier transform infrared (FTIR) spectroscopy is a powerful method to study structural changes and was applied to several LOV proteins (15-22) in the past, to elucidate the signal transfer mechanism of plant-type phototropins (20, 21) as well as of their bacterial analogues, like YtvA from *Bacillus subtilis* (16). These studies agree well with previous NMR experiments (23) and demonstrate that the J_{α}-helix, which is a conserved structural element linking the LOV and the kinase domain, unfolds in full-length phototropin1 upon light absorption (21), thereby activating the kinase domain. However, the activation of the kinase domain is neither accompanied by protonation changes nor changes in the strength of the hydrogen bond network of carboxylic side chains (21). Recent studies showed that YtvA is a dimer independent on its activation state (24, 25). However, size exclusion chromatography (SEC) and circular dichroism (CD) spectroscopy on aureochrome 1 demonstrated that dimerization of

the LOV domains upon light illumination (26, 22) leads to activation of the sensor domain (27). Dimerization and structural changes like α-helical unfolding may also play a role in the signal transfer of mPAC as its adenylyl cyclase domain can only react as a dimer. Whether this dimerization is induced by the presence of the LOV domain has so far not been clarified.

In this study, we characterize the kinetic and structural properties of the recently discovered photo-activated adenylyl cyclase mPAC. The UV/Vis absorption spectrum indicates a LOV1 like domain of mPAC. Determination of kinetics of the decay of the triplet state identify a significant shorter life time of about 650 ns in comparison to other LOV domains (typically about 2 µs), while the decay of the adduct state is with about 8 s within the usual range. Furthermore, the steady state light-induced FTIR difference spectroscopy provides molecular insight into the structural changes associated with the conversion into the putative signaling state LOV_{390}.

MATERIAL AND METHODS

Expression and Purification of wild-type mPAC and the Y476F variant

Protein expression and purification was performed as described (7). Briefly, *E.coli* RP were grown in dYT media. Expression was induced by 0.4 mM IPTG and maintained at 18 °C for 48 h at 400 rpm in the dark. Cells were harvested by centrifugation at 5700xg for 25 min. The pellet was resuspended in lysis buffer (100 mM Tris pH 8, 600 mM NaCl, 10 % Glycerol, 500 µM PMSF). Subsequently, cells were disrupted by two passages through a valve with 1.7 bar (TS Series Benchtop, Costant System). Centrifugation at 22000xg for 30 min then separated the cell debris from the soluble fraction. The supernatant was subjected to affinity chromatography via a Ni-NTA column (about 3 ml) that was equilibrated with lysis buffer. The column was washed with 10 ml each of the washing buffers A and B (50 mM Tris pH 8, 200 mM NaCl, 5 % Glycerol, 10 mM (A) and 20 mM (B) imidazole), followed by protein elution with 10 ml of elution buffer (50 mM Tris pH 8, 200 mM NaCl, 5 % Glycerol and 130 mM imidazole). After chromatography, 4 mM DTT was added to each fraction to avoid aggregation of the protein. For a second purification step, the combined mPAC containing fractions were loaded on SEC (Sephadex 25) column operated by an Äkta avant 25 (GE healthcare). Fractions containing pure mPAC were concentrated and stored in a final buffer (50 mM Tris pH 8, 200 mM NaCl, 5 % glycerol, 3 mM DTT).

Site-specific mutation was inserted by polymerase chain reaction (PCR) using the QuikChange® manual (Stratagene). As primers were used GGA AAA GGG GAA ATG ATC AAC TTT TGG CTG GTT GGG AAG CAG (forward) and CTG CTT CCC AAC CAG CCA AAA GTT GAT CAT TTC CCC TTT TCC (backward). The purification was performed accordingly to the wt and with similar yields.

Flash photolysis experiments

Purified mPAC was diluted to a concentration of 60 µM dissolved in 50 mM Tris pH 8, 200 mM NaCl, 5 % Glycerol, 3 mM DTT). The sample was excited by a short pulse from a Nd:YAG driven OPO laser system (pulse length at 475 nm was 10 ns, energy density of 2.5 mJ/cm^2, one pulse every 60 seconds). Flash photolysis experiments in the UV/Vis range were performed on two time scales:

the faster time range (<300 µs) was recorded with a Xe arc lamp as light source in pulsed mode and the slower time scale (>30 µs) was detected with the lamp in continuous wave operation. Both traces were averaged on a quasi-logarithmic time-scale and merged to yield time traces covering the time range from 50 ns to 50 s. Ten kinetic traces were averaged at each selected wavelength.

For the kinetics in dependence of imidazole, an appropriate volume of concentrated imidazole solution (8 M at pH 8) was added to the sample. After mixing, the fast and slow kinetics were recorded at 390 nm as just described.

FTIR spectroscopy

Light-induced FTIR difference spectroscopy was performed as previously described (15). Briefly, the sample was transferred in 10 mM Tris pH 8, 100 mM NaCl, 1 mM DTT buffer and dried on a BaF_2 window by a gentle stream of dry air. The protein film was rehydrated with the saturated vapor phase of a glycerol/water mixture (1:1 wt/wt). Sample hydration was sufficient, as deduced from the IR absorption in the O-H stretching range (at around 3,300 cm^{-1}). Sample excitation was performed by the same LED as for the UV/Vis experiments (see above). Infrared experiments were performed on a Vertex 80v spectrometer (Bruker Optics, Ettlingen, Germany). FTIR difference spectra were calculated by subtraction of the dark state spectra from the spectra recorded under photo stationary conditions. Spectra were recorded at a spectral resolution of 4 cm^{-1} and represent the average of 2024 scans. Data analysis was performed with OriginPro 8.1G from Origin Lab, while fitting was done in OPUS5.5 from Bruker Software.

RESULTS

UV/Vis absorption spectroscopy

The LOV domain of mPAC binds non-covalently flavin mononucleotide (FMN) as cofactor. FMN shows a typical absorption spectrum in the blue around 450 nm with vibrational fine structure at 423 and 474 nm (Fig. 1). The absorption in the UVA region (315 to 400 nm) of protein-bound FMN is strongly influenced by the amino acid surrounding as shown in recent studies (28). mPAC exhibits a

double peak in this region similar to the LOV1 domain of phototropin. The vibrational fine structure becomes clearly visible after size-exclusion chromatography (grey trace in Fig. 1). Ni-NTA affinity purification resulted in a sample with a ratio of 27.3 A_{280}/A_{450} nm (black trace). Size exclusion chromatography significantly improved the purity as inferred from an A_{280}/A_{450} ratio of 10.3. Considering the theoretical ratio of 7.6 for a fully assembled protein (7), the chromophore loading of mPAC is about 70 % which agrees well with previously reported results (7).

Pulsed laser excitation of mPAC results in a photocycle with two distinctly different intermediates. The triplet state is characterized by three absorption bands at 390, 660 and 715 nm. The kinetics of formation and decay of the intermediates were followed at 20 °C (Fig. 2). Assuming single exponential behavior, the triplet decays with time constants of 790±20 ns (660 nm) or 640±15 ns (715 nm). As the absorption at 390 nm is also characteristic to the adduct state, the time trace at 390 nm reflects two clearly separated decays with time constants of 570±11 ns for LOV_{715} and 8.2±0.5 s for LOV_{390}. The latter decays directly into the initial ground state as inferred from the identical time constant of 8.2±0.2 s for the recovery kinetics observed at 450 nm. It should be pointed out here that the relatively long recovery time of mPAC is challenging for the ns flash photolysis experiments as the repetition rate was one pulse per minute. Care was taken to avoid accumulation of the photoproduct that might interfere with the analysis of the dark state by shading effects or unintended photochemistry of the photoproduct. The differences in the decay of the triplet state detected at different wavelengths are not significant. The average time constant is 656 (±81) ns.

It was reported for other LOV domains that the presence of imidazole accelerates the thermal decay of the adduct state via a base-catalyzed mechanism (29). In this mechanism, imidazole acts as a base to accept the proton from the N5 of the isoallaxazine ring of FMN as a prerequisite for bond cleavage in the thio-adduct of FMN with the sulfhydryl of the reactive cysteine. In fact, also for mPAC the influence of imidazole on the kinetics of the recovery of the ground state could be detected (Fig. 3). While the decay of the triplet state is not influenced by the imidazole concentration, the decay of the adduct state (= reformation of the parental state) is two-fold accelerated at concentrations of 500 mM.

208 *FTIR differences in the 1800-900 cm^{-1} region*

209 UV/Vis spectroscopy is an excellent tool to trace the electronic changes after light excitation of the
210 chromophore FMN. The succeeding structural changes including the apo-protein, however, are best
211 studied by FTIR spectroscopy. Light-induced differences are recorded under photo-stationary
212 conditions to reveal the molecular changes between the ground and the long-lived adduct state. The
213 resulting spectra in the region between 1800 and 900 cm^{-1} (Fig. 4) include the amide I and II region,
214 which is indicative to structural changes on the protein backbone, as well as the vibrations of most
215 amino acids side chains and the FMN chromophore. Like in other LOV domains, the FTIR difference
216 spectrum is dominated by the vibrational bands of the chromophore because the formation of the
217 adduct state induces a large change in the dipole moment of FMN, and as known from other LOV
218 domains, secondary structure changes of the protein are often of minor intensity. Bands of the adduct
219 state at 1726, 1688, 1655, 1625, 1541, 1520, 1427, 1367, 1331, 1304, 1190 and 1092 cm^{-1} (Fig. 4)
220 appear after blue-light excitation (positive absorbance), while bands at 1714, 1695, 1676, 1583, 1552,
221 1352, 1273, 1248, 1223 and 1082 cm^{-1} disappear (negative absorbance) and, thus, correspond to the
222 ground state. The band assignment is based on comparison to LOV1 from phototropin-1 from
223 *Chlamydomonas reinhardtii* (15). The region between 1800 and 1000 cm^{-1} provides additional
224 information when the spectra of mPAC in H_2O, D_2O and $H_2{}^{18}O$ are compared (see Fig. 4). The $H_2{}^{18}O$
225 exchange (Fig. 4, lower trace) yields a change in intensity of the band at 1655/1641 cm^{-1}, however, no
226 further significant changes were observed. In contrast, the D_2O exchange (Fig. 4, upper trace) shows
227 more drastic changes. In the LOV_{390} intermediate several bands are shifted. One band in the amide I
228 region at 1655 cm^{-1} is shifted upwards to 1660 cm^{-1}, while another band at 1685 cm^{-1} is slightly
229 downshifted to 1683 cm^{-1}. Furthermore, the positive band at 1520 cm^{-1} disappears almost completely.
230 The positive bands at 1427, 1376, and 1304 cm^{-1} also disappear, similar as observed before for the
231 phot-LOV1 domain (15). The negative bands at 1273, 1248, and 1223 cm^{-1} underlie the strongest
232 changes confirming the assignment to potent indicators for hydrogen bond interactions (15), while the
233 negative band at 1082 cm^{-1} vanishes completely. In addition, the bands at 1352, 1131, and 1194 cm^{-1}
234 are shifted by a few wavenumbers.

235

FTIR spectra in the S-H stretching region

As the formation of the adduct state requires breakage of the sulfhydryl bond of the involved cysteine residue, the S-H stretching vibration represents a local sensor of the structure surrounding the chromophore. The light-dark difference spectrum of mPAC (Fig. 5) shows the typical negative band recorded in all LOV domains. This band is assigned to cysteine 197 based on the homology to other LOV domains. The frequency of the S-H stretching vibration is decreased in relation with an increase in hydrogen donating character of the S-H moiety. mPAC shows a negative difference band at 2573 cm^{-1} identical to the LOV2 domain of phototropin-1 (16). The band displays a shoulder at the lower frequency end which is fitted by a second band with a frequency of 2557 cm^{-1}. The same was observed for the S-H stretching band of the homologous cysteine residue of YtvA and the LOV1 domain of phototropin with minima at 2569/2561 and 2570/2562 cm^{-1}, respectively (16). In contrast, the S-H stretching vibration of aureochrome 1 is sharp at a minimum of 2563 cm^{-1} (redrawn from (30)). The two side bands in LOV1 and YtvA correspond to the two possible rotamer configurations of the respective cysteines (C57 in LOV1 and C62 in YtvA). The occupancy of the two rotamers was determined to 70 and 30 % from the crystal structure of YtvA (27) and LOV1 (27, 31). In close agreement, the band areas of the fitted Gaussians in the FTIR spectrum revealed a distribution of 63 and 37 % for YtvA and 74 and 26 % for LOV1 (16). Spectral analysis of the S-H stretching band of mPAC revealed with 90 and 10 % only a minor contribution of the other rotamer. As an additional observation the frequency of the shoulder is shifted by 4-5 cm^{-1} in comparison to other LOV domains.

FTIR Spectra in the 3800-2800 cm^{-1} region

This frequency range is typical for single bond stretches (predominantly O-H, N-H and C-H in proteins). This amide A region is not only sensitive to changes of the protein conformation but also to changes in the hydrogen-bonded network. In the LOV_{390} minus LOV_{450} difference spectra of phy3-LOV2, aureochrome 1 and YtvA a positive band in the region from 3620 to 3640 cm^{-1} is observed that was assigned to a weakly hydrogen bonded internal water molecule in close vicinity to the FMN (32). Formation of adduct state breaks the hydrogen bond of the FMN to this nearby water molecule. Thus, the frequency of the O-H stretching vibration shifts from lower to higher wavenumbers and appear as

a positive band in the spectrum. However, mPAC shows an additional positive band in this region at 3674 cm^{-1}. To clarify if this band belongs as well to an O-H stretching mode of a water molecule, measurements in D_2O and $H_2{}^{18}O$ were performed. The resulting difference spectra of the bands influenced by the exchange are shown in Fig. 7. The exchange of water by D_2O shifts the S-H vibration from 2572 to 1870 cm^{-1} (S-D vibration). Furthermore the O-H stretching vibrations occurring at around 3650 cm^{-1} are downshifted to around 2700 cm^{-1} along with a decrease in extinction coefficient.

As expected, the S-H stretching vibration is not changed in $H_2{}^{18}O$ whereas the band at 3632 cm^{-1} is downshifted by 10 cm^{-1} characteristic for the O-H stretching vibrational band of a water molecule after $^{16}O/^{18}O$ exchange. The band at 3674 cm^{-1} splits into two upon $H_2{}^{18}O$ exchange, showing a band at 3663 cm^{-1} with a shoulder at 3674 cm^{-1}. This shows that the band at 3674 cm^{-1} is composed of two overlapping O-H stretching vibrations, only one arising from an intrinsic water molecule. The frequency of the other band is indicative for the phenolic side chain vibration of a tyrosine residue. Due to the fact that this band appears in mPAC only, it is reasonable to assume that it arises from a residue in the adenylyl cyclase domain. First, we generated a T318A variant because T318 is directly involved in ATP binding by forming hydrogen bonds to the ribose. However, the FTIR difference spectrum was exactly the same as for the wild type (data not shown). The sequence alignment using PHYRE2 (33) showed a conserved tyrosine residue at the C-terminus of the cyclase domain (Fig. 8). To gauge the putative role of this residue, we generated the Y476F mutant. The UV/Vis absorption spectrum and kinetics of the Y476F variant are identical to the wild type (data not shown). The FTIR spectra of the wild type and the variant are identical as well. However, if H_2O is replaced by $H_2{}^{18}O$ the same shift for the water bands appear but the shoulder at 3674 cm^{-1} disappears (Fig. 9). This experiment clearly assigns the band at 3674 cm^{-1} to the O-H stretching vibration of the phenolic side chain of Y476.

DISCUSSION

The photoreaction of the new adenylyl cyclase mPAC from *Microcoleus chthonoplastes* was studied by molecular spectroscopy. The visible spectrum, which reveals a double band feature in the UVA region, shows that the LOV domain of mPAC is similar to LOV1 from phototropin (28, 34). This finding is reflected by lacking of the otherwise conserved residues T418 and N425 in *Avena sativa* phot-LOV2 (A162 and M169 in mPAC), involved in determination of the spectral feature in the UVA region.

Time-resolved flash photolysis recorded the kinetics of the triplet decay with a time constant of 656 (±81) ns as one of the fastest lifetimes for LOV domains. Only for phot-LOV1 from *Chlamydomonas reinhardtii,* a time constant of 800 ns for a parallel formed triplet state LOV_{715a} was reported (11). Usually, the decay of the triplet state is a few µs, like for phot1 LOV1 (4 µs), LOV2 (1.9 µs), YtvA (2 µs) and aureochrome 1 (1.4 µs) (11, 14, 13). The back reaction at 20 °C to the initial ground state was determined with a time constant of 8.2 s. This value is in the range of the previously reported lifetime of 16 s (7).

The decay of the adduct state requires breakage of the S-C(4a) bond and proton transfer from N(5). For other studied LOV domains this reaction can be accelerated by a base-catalyzed mechanism employing imidazole (29). However, mPAC does not show significant changes in the kinetics of the dark state recovery in the presence or absence of imidazole, except for very high imidazole concentrations of 500 mM and 1 M the time constant increases to 4.5 and 2.1 s, respectively. This corresponds to a 2-fold and 4-fold acceleration. However, other LOV domains like aureochrome 1 from the Diatom *Phaeodactylum tricornutum* already show a 20-fold acceleration of ground-state recovery at imidazole concentrations of 1 mM (22) and a 30-fold increase was observed at 50 mM imidazole for LOV2 domain of *Avena sativa* phototropin-1 (29). Recent studies pointed out the importance of a threonine residue close to the FMN binding pocket in some fungal and bacterial LOV proteins (T101 in ENV1 and T27 in McLOVr) in the recruitment and dynamics of internal water molecules (35, 36). In mPAC, however, this residue is replaced by the hydrophobic valine, like in several other LOV domains. Furthermore the role of this threonine is quite diverted because mutation into isoleucine made the binding pocket of ENV1 less accessible for solvent molecules while the same

mutation in McLOV lead to an increase in the solvent-accessibility factor and made the adduct decay sensitive to imidazole. Our finding that the adduct decay of mPAC is insensitive to low imidazole concentration (up to 100 mM) shows that its LOV domain is more similar to that of ENV1 T101I with an ordered structure regardless of water occupancy (35).

The light-induced FTIR difference spectrum demonstrates the high similarity of the mPAC domain to other LOV domains. The spectrum shares the typical FMN bands and also reveals the expected shifts due to H/D exchange. The difference bands in the amide I region around 1650 cm^{-1} are quite small in comparison to other LOV domains like aureochrome 1. Thus, minor structural changes due to light activation are considered. For further investigation of the reaction mechanism, size exclusion chromatography measurements are future tasks.

The S-H stretching region also reveals the typical negative peak indicative for the disappearance of sulfhydryl group, which we assigned to C197. This peak is asymmetric and can be fitted by two Gaussians resulting with peaks at 2557 and 2573 cm^{-1}. The relative area of the two vibrational bands is 12 and 88 %. Thus, two rotamers of the reactive cysteine are present in mPAC as was also found in other LOV domains (11, 16). In contrast to LOV1 from phototropin, the kinetics of the triplet state decay is mono-exponential and does not provide any evidence for a second species.

A positive band at 3632 cm^{-1} is found in the water and amide A region for mPAC that is assigned to an intrinsic water molecule analogous to other LOV domains (32). However, an additional positive band was identified at 3674 cm^{-1} which is unique for mPAC. Tentatively been assigned to an alcoholic side chain, the mutation of tyrosine 476 (Y476F) clearly proved that this band is composed by two overlapping bands, one from another intrinsic water molecule and the other part arising from the phenolic O-H stretch of Y476. Sequence alignment of the mPAC adenylyl cyclase domain with others shows that the tyrosine residue is conserved in most of the domains or it is conservatively replaced by a phenylalanine. This conservation explains the fully functional variant Y476F and underpins the relevance of this residue. The structure of the adenylyl cyclase domain of mPAC was modeled using SWISS-MODEL (37)(38) and the crystal structure of CyaC (PDB entry: 1WC5) as a template. However, the resulting model didn't give insights into the position and function of Y467 because it wasn't included in the model. Using PHYRE2 (33) as a modeling tool resulted in a very similar

structure as obtained from SWISS-MODEL but showed the C-terminus as an extension of two sheets to the core β-sheet. Y476 is located in this β-sheet facing the α-helix that contains the conserved residues N429 and R433 facing the dimer interface and involved in ATP binding (α-phosphate and ribose) (37). In the model, the distance (9.4 Å) is too far to form a hydrogen bond but the cavity in between these residues seems sufficiently large to accommodate one (or more) water molecule(s). This structure could explain the second water molecule that was observed in the FTIR difference spectra. However, this models can provide only a very coarse view. To further investigate the importance of this tyrosine residue, experimental techniques that are sensitive to the oligomeric state in the light and dark as well as activity assays need to be applied (39).

The LOV domain of mPAC from *Microcoleus chthonoplastes* exhibits most features identified also in other LOV domains with steady-state (32, 40, 16, 41, 42, 30, 43) and time-resolved spectroscopy (20, 44). The remarkably rapid triplet decay, so far the fastest observed ever in LOV domains, must be ascribed to the protein pocket which destabilizes the triplet state of the flavin chromophore. This suggestion is based on the rationale that the rate of triplet decay is controlled by the accessibility to molecular oxygen which quenches the triplet state (destabilization). The finding that the overall changes between the dark and the lit state are marginal is not surprising as it was already determined for many LOV domains that light-induced conformational changes are small, and the signal travels mostly through a rearrangement of hydrogen bonds, induced by rotation of asparagine and glutamine side chains (21, 42). Even changes in the AC domain must not be considered large, as the activation mechanism might not include large secondary structural changes, but instead a rearrangement of two AC moieties relative to each other, as it is known that the active site of ACs is formed at the interface of two monomers (42).

The finding of a LOV domain (instead of the BLUF domains described so far for PAC) as the light-regulating domain seemed at first glance advantageous, as many LOV domains show a stable photoproduct state, i.e., a retarded recovery of the parental state, a property advantageous for optogenetic applications. In mPAC, however, the decay of the photoproduct is fairly fast, requiring similarly as in the BLUF domain regulated ACs, intense exposure of the cells or tissue to blue light. Extended mutagenesis studies in relation to sequence alignments might help identifying amino acids

that stabilize the photoproduct state without interfering with the communication between the LOV and the AC domain.

ACKNOWLEDGMENT

This work was supported by a grant from the Deutsche Forschungsgemeinschaft (DFG) within the Forschergruppe 1279 ‘‘Protein-based photoswitches as optogenetic tools’’ to J.H.

REFERENCES

1. Losi, A. and W. Gärtner (2012) The evolution of flavin-binding photoreceptors: an ancient chromophore serving trendy blue-light sensors. *Annu. Rev. Plant Biol.* **63,** 49-72.
2. Iseki, M., S. Matsunaga, A. Murakami, K. Ohno, K. Shiga, K. Yoshida, M. Sugai, T. Takahashi, T. Hori and M. Watanabe (2002) A blue-light-activated adenylyl cyclase mediates photoavoidance in Euglena gracilis. *Nature* **415,** 1047-1051.
3. Schröder-Lang, S., M. Schwärzel, R. Seifert, T. Strünker, S. Kateriya, J. Looser, M. Watanabe, U. B. Kaupp, P. Hegemann and G. Nagel (2007) Fast manipulation of cellular cAMP level by light in vivo. *Nat Methods* **4,** 39-42.
4. Looser, J., S. Schröder-Lang, P. Hegemann and G. Nagel (2009) Mechanistic insights in light-induced cAMP production by photoactivated adenylyl cyclase alpha (PACalpha). *Biol Chem* **390,** 1105-1111.
5. Yoshikawa, S., T. Suzuki, M. Watanabe and M. Iseki (2005) Kinetic analysis of the activation of photoactivated adenylyl cyclase (PAC), a blue-light receptor for photomovements of Euglena. *Photochem Photobiol Sci* **4,** 727-731.
6. Stierl, M., P. Stumpf, D. Udwari, R. Gueta, R. Hagedorn, A. Losi, W. Gärtner, L. Petereit, M. Efetova, M. Schwarzel, T. G. Oertner, G. Nagel and P. Hegemann (2011) Light modulation of cellular cAMP by a small bacterial photoactivated adenylyl cyclase, bPAC, of the soil bacterium Beggiatoa. *J Biol Chem* **286,** 1181-1188.
7. Raffelberg, S., L. Wang, S. Gao, A. Losi, W. Gärtner and G. Nagel (2013) A LOV-domain-mediated blue-light-activated adenylate (adenylyl) cyclase from the cyanobacterium Microcoleus chthonoplastes PCC 7420. *Biochem J* **455,** 359-365.
8. Taylor, B. L. and I. B. Zhulin (1999) PAS domains: Internal sensors of oxygen, redox potential, and light. *Microbiol.Mol.Biol.Rev.* **63,** 479-506.
9. Swartz, T. E., S. B. Corchnoy, J. M. Christie, J. W. Lewis, I. Szundi, W. R. Briggs and R. A. Bogomolni (2001) The photocycle of a flavin-binding domain of the blue light photoreceptor phototropin. *J Biol.Chem.* **276,** 36493-36500.
10. Bauer, C., C. R. Rabl, J. Heberle and T. Kottke (2011) Indication for a radical intermediate preceding the signaling state in the LOV domain photocycle. *Photochem Photobiol* **87,** 548-553.
11. Kottke, T., J. Heberle, D. Hehn, B. Dick and P. Hegemann (2003) Phot-LOV1: Photocycle of a Blue-Light Receptor Domain from the Green Alga Chlamydomonas reinhardtii *Biophys J* **84,** 1192-1201.

12. Christie, J. M., M. Salomon, K. Nozue, M. Wada and W. R. Briggs (1999) LOV (light, oxygen, or voltage) domains of the blue-light photoreceptor phototropin (nph1): binding sites for the chromophore flavin mononucleotide. *Proc Natl Acad Sci U S A* **96,** 8779-8783.
13. Losi, A., B. Quest and W. Gärtner (2003) Listening to the blue: the time-resolved thermodynamics of the bacterial blue-light receptor YtvA and its isolated LOV domain. *Photochem Photobiol Sci* **2,** 759-766.
14. Nakasone, Y., T. Eitoku, D. Matsuoka, S. Tokutomi and M. Terazima (2006) Kinetic measurement of transient dimerization and dissociation reactions of Arabidopsis phototropin 1 LOV2 domain. *Biophys J* **91,** 645-653.
15. Ataka, K., P. Hegemann and J. Heberle (2003) Vibrational Spectroscopy of an Algal Phot-LOV1 Domain Probes the Molecular Changes Associated with Blue-Light Reception. *Biophysical Journal* **84,** 466-474.
16. Bednarz, T., A. Losi, W. Gartner, P. Hegemann and J. Heberle (2004) Functional variations among LOV domains as revealed by FT-IR difference spectroscopy. *Photochem Photobiol Sci* **3,** 575-579.
17. Sato, Y., T. Iwata, S. Tokutomi and H. Kandori (2005) Reactive cysteine is protonated in the triplet excited state of the LOV2 domain in Adiantum phytochrome3. *J.Am.Chem.Soc.* **127,** 1088-1089.
18. Iwata, T., D. Nozaki, Y. Sato, K. Sato, Y. Nishina, K. Shiga, S. Tokutomi and H. Kandori (2006) Identification of the C=O Stretching Vibrations of FMN and Peptide Backbone by (13)C-Labeling of the LOV2 Domain of Adiantum Phytochrome3. *Biochemistry* **45,** 15384-15391.
19. Kikuchi, S., M. Unno, K. Zikihara, S. Tokutomi and S. Yamauchi (2009) Vibrational assignment of the flavin-cysteinyl adduct in a signaling state of the LOV domain in FKF1. *J Phys Chem B* **113,** 2913-2921.
20. Pfeifer, A., T. Majerus, K. Zikihara, D. Matsuoka, S. Tokutomi, J. Heberle and T. Kottke (2009) Time-resolved Fourier transform infrared study on photoadduct formation and secondary structural changes within the phototropin LOV domain. *Biophys. J.* **96,** 1462-1470.
21. Pfeifer, A., T. Mathes, Y. Lu, P. Hegemann and T. Kottke (2010) Blue light induces global and localized conformational changes in the kinase domain of full-length phototropin. *Biochemistry* **49,** 1024-1032.
22. Herman, E., M. Sachse, P. G. Kroth and T. Kottke (2013) Blue-Light-Induced Unfolding of the Jα Helix Allows for the Dimerization of Aureochrome-LOV from the Diatom Phaeodactylum tricornutum. *Biochemistry* **52,** 3094-3101.
23. Harper, S. M., L. C. Neil and K. H. Gardner (2003) Structural basis of a phototropin light switch. *Science* **301,** 1541-1544.
24. Lee, R., J. Gam, J. Moon, S. G. Lee, Y. G. Suh, B. J. Lee and J. Lee (2015) A critical element of the light-induced quaternary structural changes in YtvA-LOV. *Protein Sci* **24,** 1997-2007.
25. Jurk, M., M. Dorn, A. Kikhney, D. Svergun, W. Gartner and P. Schmieder (2010) The switch that does not flip: the blue-light receptor YtvA from Bacillus subtilis adopts an elongated dimer conformation independent of the activation state as revealed by a combined AUC and SAXS study. *J Mol Biol* **403,** 78-87.
26. Buttani, V., A. Losi, T. Eggert, U. Krauss, K. E. Jaeger, Z. Cao and W. Gartner (2007) Conformational analysis of the blue-light sensing protein YtvA reveals a competitive interface for LOV-LOV dimerization and interdomain interactions. *Photochem Photobiol Sci* **6,** 41-49.
27. Moglich, A. and K. Moffat (2007) Structural basis for light-dependent signaling in the dimeric LOV domain of the photosensor YtvA. *Journal.Of.Molecular.Biology.* **373,** 112-126.
28. Raffelberg, S., A. Gutt, W. Gärtner, C. Mandalari, S. Abbruzzetti, C. Viappiani and A. Losi (2013) The amino acids surrounding the flavin 7a-methyl group determine the UVA spectral features of a LOV protein. *Biol Chem* **394,** 1517-1528.
29. Alexandre, M. T., J. C. Arents, R. van Grondelle, K. J. Hellingwerf and J. T. Kennis (2007) A base-catalyzed mechanism for dark state recovery in the Avena sativa phototropin-1 LOV2 domain. *Biochemistry* **46,** 3129-3137.

30. Kerruth, S., K. Ataka, D. Frey, I. Schlichting and J. Heberle (2014) Aureochrome 1 illuminated: structural changes of a transcription factor probed by molecular spectroscopy. *Plos One* **9,** e103307.
31. Fedorov, R., I. Schlichting, E. Hartmann, T. Domratcheva, M. Fuhrmann and P. Hegemann (2003) Crystal Structures and Molecular Mechanism of a Light-Induced Signaling Switch: The Phot-LOV1 Domain from Chlamydomonas reinhardtii *Biophysical Journal* **84,** 2474-2482.
32. Iwata, T., D. Nozaki, S. Tokutomi, T. Kagawa, M. Wada and H. Kandori (2003) Light-induced structural changes in the LOV2 domain of Adiantum phytochrome3 studied by low-temperature FTIR and UV-visible spectroscopy. *Biochemistry* **42,** 8183-8191.
33. Kelley, L. A., S. Mezulis, C. M. Yates, M. N. Wass and M. J. Sternberg (2015) The Phyre2 web portal for protein modeling, prediction and analysis. *Nat Protoc* **10,** 845-858.
34. Salomon, M., J. M. Christie, E. Knieb, U. Lempert and W. R. Briggs (2000) Photochemical and mutational analysis of the FMN-binding domains of the plant blue light receptor, phototropin. *Biochemistry* **39,** 9401-9410.
35. Lokhandwala, J., Y. d. l. V. R. I. Silverman, H. C. Hopkins, C. W. Britton, A. Rodriguez-Iglesias, R. Bogomolni, M. Schmoll and B. D. Zoltowski (2016) A Native Threonine Coordinates Ordered Water to Tune Light-Oxygen-Voltage (LOV) Domain Photocycle Kinetics and Osmotic Stress Signaling in Trichoderma reesei ENVOY. *J Biol Chem* **291,** 14839-14850.
36. El-Arab, K. K., A. Pudasaini and B. D. Zoltowski (2015) Short LOV Proteins in Methylocystis Reveal Insight into LOV Domain Photocycle Mechanisms. *Plos One* **10,** e0124874.
37. Bordoli, L., F. Kiefer, K. Arnold, P. Benkert, J. Battey and T. Schwede (2009) Protein structure homology modeling using SWISS-MODEL workspace. *Nat Protoc* **4,** 1-13.
38. Biasini, M., S. Bienert, A. Waterhouse, K. Arnold, G. Studer, T. Schmidt, F. Kiefer, T. Gallo Cassarino, M. Bertoni, L. Bordoli and T. Schwede (2014) SWISS-MODEL: modelling protein tertiary and quaternary structure using evolutionary information. *Nucleic Acids Res* **42,** W252-258.
39. Liu, Y., A. E. Ruoho, V. D. Rao and J. H. Hurley (1997) Catalytic mechanism of the adenylyl and guanylyl cyclases: modeling and mutational analysis. *Proc Natl Acad Sci U S A* **94,** 13414-13419.
40. Ataka, K., P. Hegemann and J. Heberle (2003) Vibrational spectroscopy of an algal Phot-LOV1 domain probes the molecular changes associated with blue-light reception. *Biophys. J.* **84,** 466-474.
41. Iwata, T., D. Nozaki, S. Tokutomi and H. Kandori (2005) Comparative investigation of the LOV1 and LOV2 domains in Adiantum phytochrome3. *Biochemistry* **44,** 7427-7434.
42. Herman, E., M. Sachse, P. G. Kroth and T. Kottke (2013) Blue-Light-Induced Unfolding of the J alpha Helix Allows for the Dimerization of Aureochrome-LOV from the Diatom Phaeodactylum tricornutum. *Biochemistry* **52,** 3094-3101.
43. Herman, E. and T. Kottke (2015) Allosterically Regulated Unfolding of the A 'alpha Helix Exposes the Dimerization Site of the Blue-Light-Sensing Aureochrome-LOV Domain. *Biochemistry* **54,** 1484-1492.
44. Thöing, C., A. Pfeifer, S. Kakorin and T. Kottke (2013) Protonated triplet-excited flavin resolved by step-scan FTIR spectroscopy: implications for photosensory LOV domains. *Physical Chemistry Chemical Physics* **15,** 5916-5926.

524 FIGURES

525

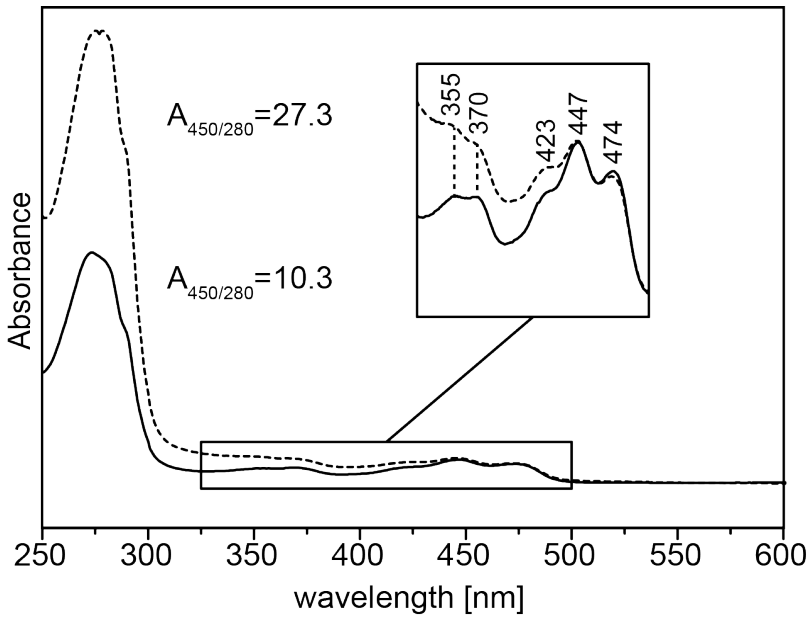

526

527 Figure 1: UV/Vis absorption spectra of mPAC before (dotted line) and after (black line) size exclusion

528 chromatography. The area between 325 and 500 nm is show as a zoom in (insert). The peaks of the

529 blue and UVB absorption of the FMN chromophore are labeled.

530

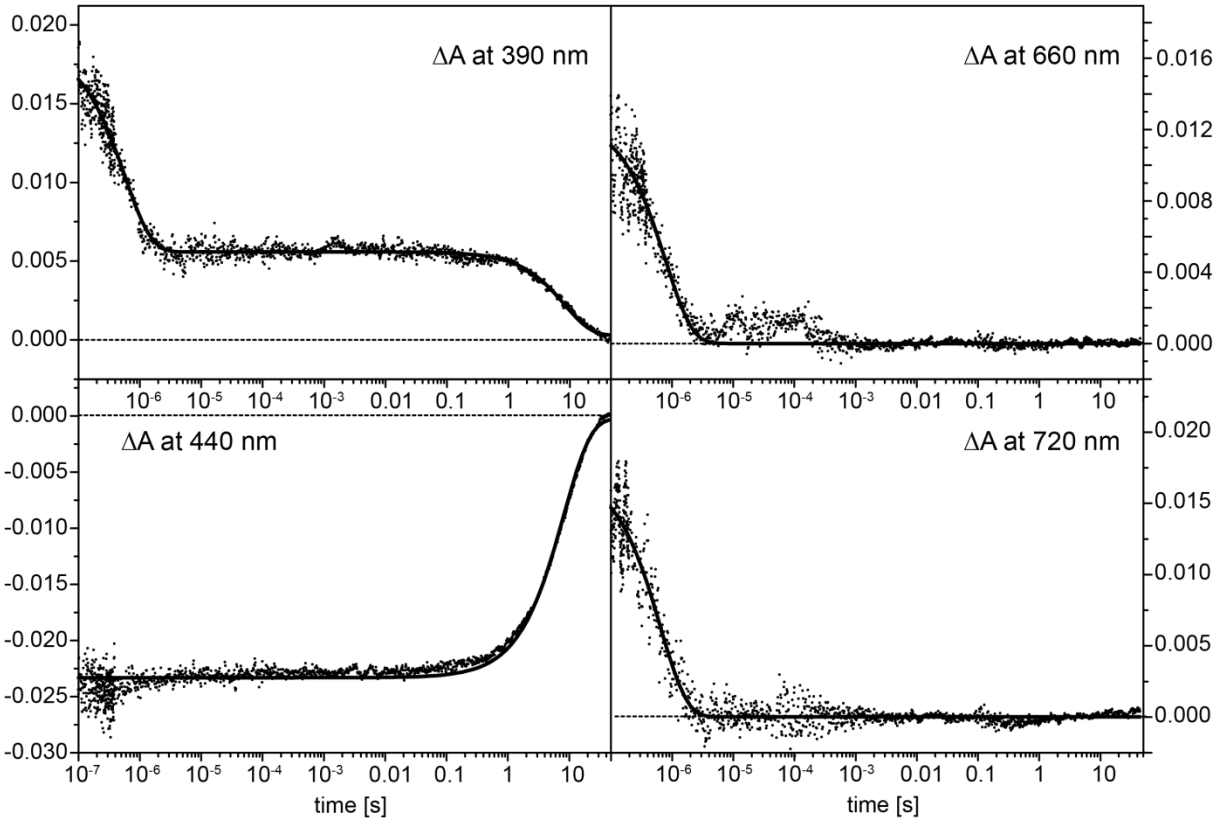

Figure 2: Time-resolved UV/vis absorption difference spectroscopy of mPAC at 390, 440, 660 and 720 nm. The data points were fitted to single exponential decays for 440, 660 and 720 nm and with two exponential decays for 390 nm (black lines). The resulting time constants for the triplet decay are 570±11, 790±20 and 640±15 ns for 390, 660 and 720 nm, respectively. The differences in the time constants are not significant, leading to an average decay time of 656 (±81) ns. The time constants for the decay of the adduct state and the recovery of the ground state were determined to be 8.2±0.5 s and 8.2±0.2 s, respectively.

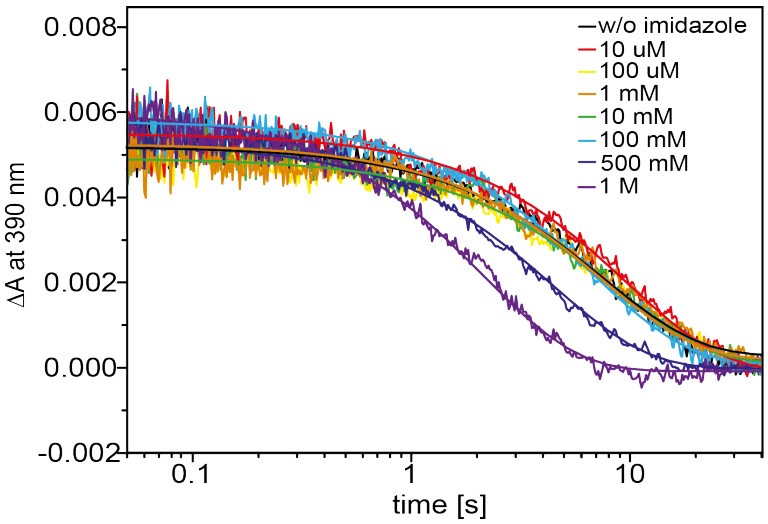

$c_{imidazole}$ [M]	τ_1 [ns]	τ_2 [s]
0	786±26	7.6±0.5
10^{-5}	659±18	9.8±0.8
10^{-4}	657±16	7.6±0.7
10^{-3}	671±18	8.4±0.7
10^{-2}	623±15	7.5±0.6
0.1	639±17	6.8±0.5
0.5	515±15	4.5±0.3
1	664±21	2.1±0.2

Figure 3: Time-resolved UV/Vis difference spectra at 390 nm of mPAC at different imidazole concentrations. The figures shows the slow time domain between 500 ms and 50 s corresponding to the decay of the adduct state. The decay of the triplet state that occurs in the µs time domain is included in the two-exponential decay fit of the data but not shown in the time trace. The corresponding time constants τ_1 and τ_2 for the triplet and adduct state, respectively, are listed in the table on the right.

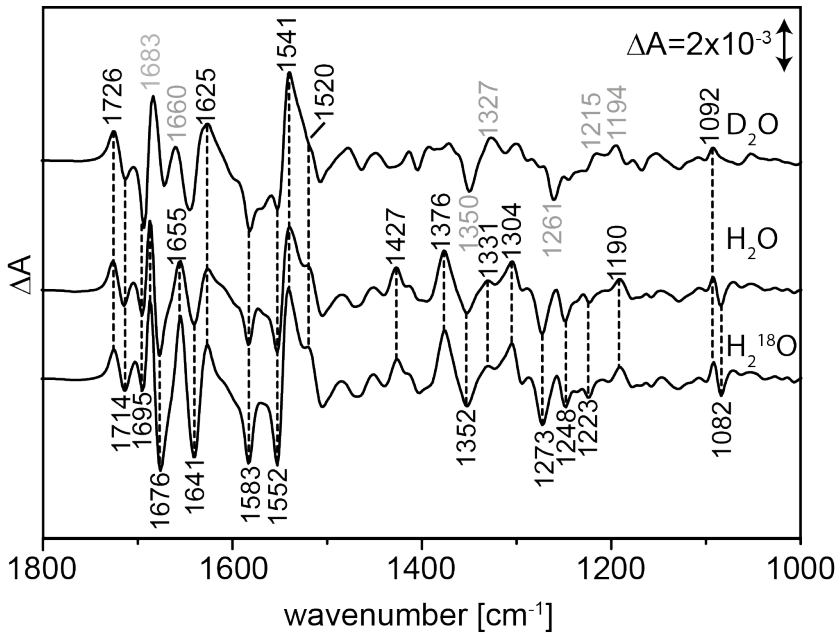

Figure 4: FTIR steady state difference spectra of mPAC with different isotope (^{2}H, ^{18}O) labeled water preparations. Similar bands in the spectra are connected with dotted lines, whereas those that differ between the spectra are labeled with corresponding wavenumbers colored in grey.

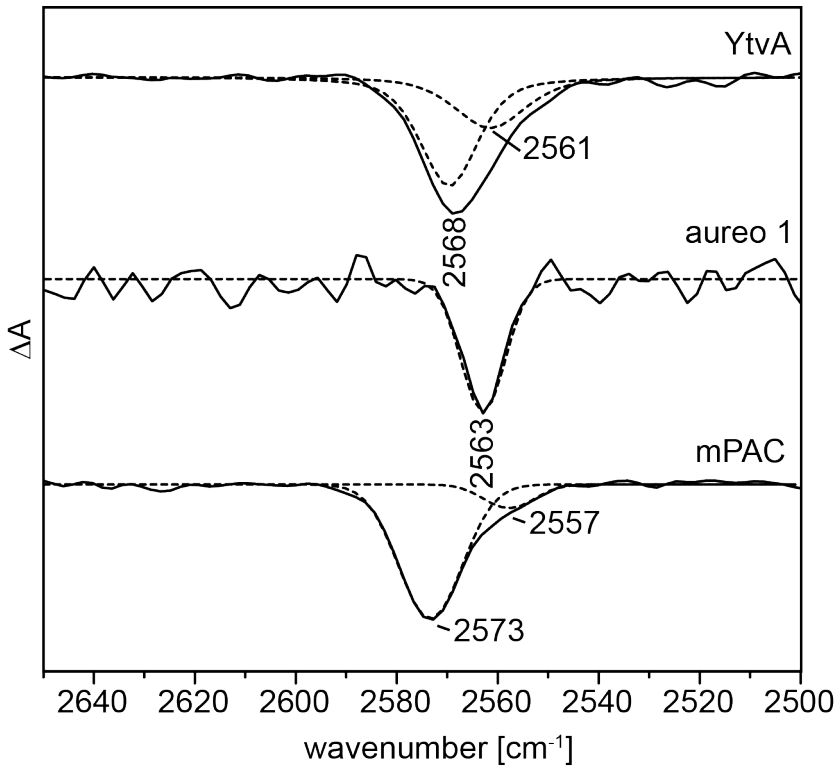

Figure 5: FTIR difference spectra of different LOV proteins in the S-H stretching region. The spectra of aureochrome 1 and YtvA are replotted from refs. (30) and (16), respectively. The dotted lines are Gaussian fits to the peaks. The peak of mPAC is fitted with two Gaussian functions with minima at 2573 and 2557 cm^{-1}.

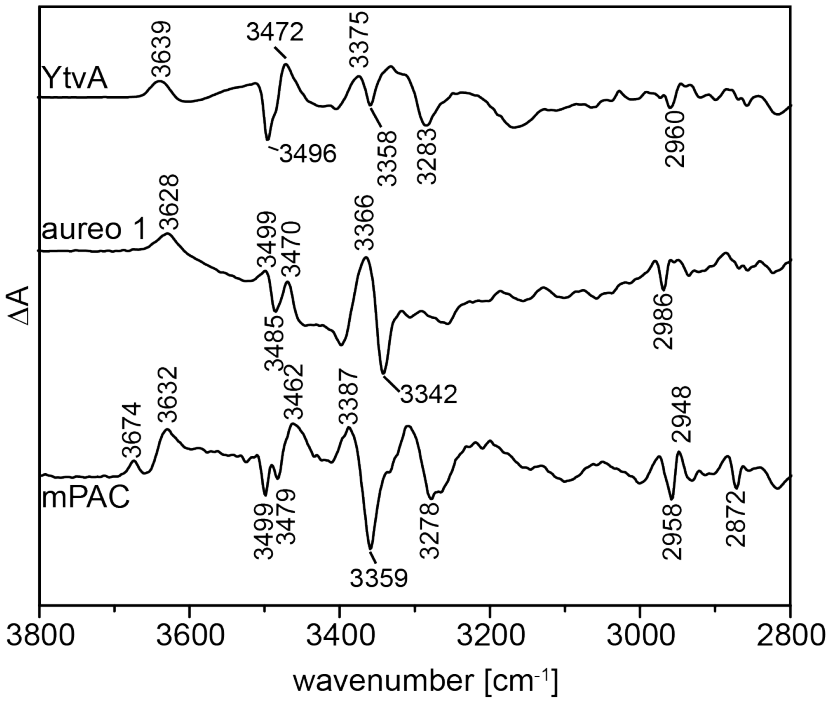

Figure 6: Light-dark FTIR difference spectra of three different LOV proteins in the 2800-3800 cm^{-1} region. The upper spectrum corresponds to YtvA (replotted from (16)), the middle one to aureochrome 1 (30) and the lower one to mPAC. The numbers indicate the band positions in cm^{-1}.

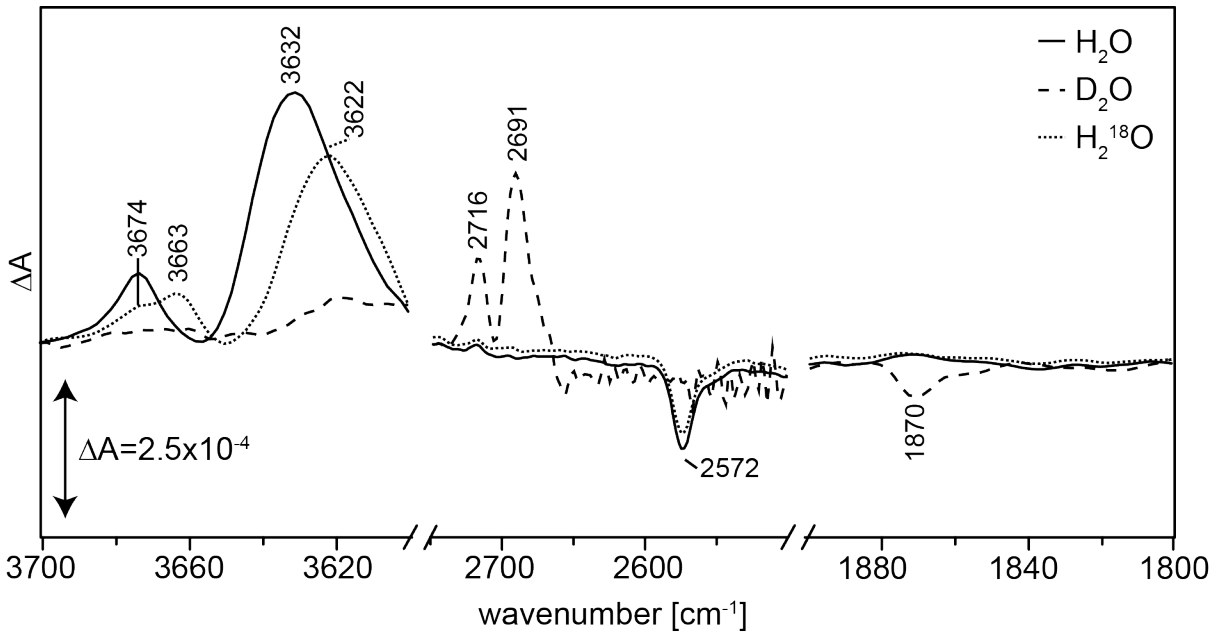

Figure 7: FTIR steady state difference spectra of mPAC with different isotope labeled water preparations. The regions typical for dangling waters (3600-3700 cm^{-1}), for S-H vibrations (2750-2500 cm^{-1}) and for S-D vibrations (1900-1800) are shown. The solid black line represents the mPAC difference spectrum in H_2O, while the dotted line corresponds to the spectrum in $H_2{}^{18}O$ and the solid grey line corresponds to the one in D_2O.

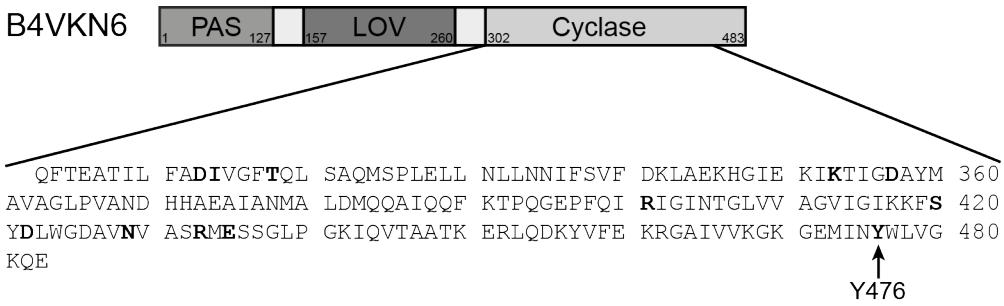

Figure 8: Schematic view of the three domains of mPAC (B4VKN6) with the detailed sequence of the adenylyl cyclase domain. The residues shown in bold are involved in ATP and ion binding (Mg^{2+}/Ca^{2+}). The crucial residue Y467 is indicated by an arrow.

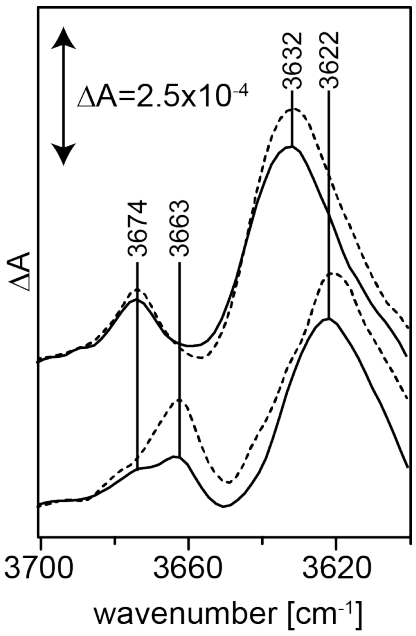

Figure 9: FTIR difference spectra of mPAC wild type (black line) and Y476F variant (red line) in H_2O (upper spectra) and $H_2{}^{18}O$ (lower spectra) in the region between 3750 and 3600 cm^{-1}. Spectra have been scaled to yield identical intensities of the S-H stretching vibration at 2572 cm^{-1}.